JPET Fast Forward. Published on November 14, 2003 as DOI:10.1124/jpet.103.060590

JPET # 60590

Investigation of the interaction of a putative allosteric modulator, SCH-202676, with M_1 muscarinic acetylcholine receptors

Alfred Lanzafame and Arthur Christopoulos

Department of Pharmacology, University of Melbourne, Parkville, 3010, Victoria, Australia

JPET Fast Forward. Published on November 14, 2003 as DOI: 10.1124/jpet.103.060590
This article has not been copyedited and formatted. The final version may differ from this version.

a) Running title: Interaction of SCH-202676 with M_1 receptors

b) Author for correspondence

Dr Arthur Christopoulos, NHMRC Senior Research Fellow, Department of Pharmacology, University of Melbourne, Grattan Street, Parkville, 3010, Victoria, Australia; Phone: +613 8344 8417; Fax: +613 8344 0241; Email: arthurc1@unimelb.edu.au.

c) Number of text pages: 32

Number of tables: 2

Number of figures: 7

Number of references: 24

Number of words in the Abstract: 249

Number of words in the Introduction: 617

Number of words in the Discussion: 1496

d) Non-standard abbreviations: ACh, acetylcholine; C_7/3-phth, heptane, 1,7-bis-(dimethyl-3'-phthalimidopropyl)-ammonium bromide; C-R, concentration-response; DMEM, Dulbecco's modified eagle medium; GPCR, G protein-coupled receptor; mAChR, muscarinic acetylcholine receptor; NMS, N-methylscopolamine; PI, phosphoinositide; SCH-202676, *N*-(2,3-diphenyl-1,2,4-thiadiazole-5-(2*H*)-ylidene) methanamine hydrobromide; TCM, ternary complex model

e) Recommended section: Cellular & Molecular

Abstract

The interaction between a novel G protein-coupled receptor modulator, *N*-(2,3-diphenyl-1,2,4-thiadiazole-5-(2*H*)-ylidene) methanamine hydrobromide (SCH-202676), and the M_1 muscarinic acetylcholine receptor (mAChR) was investigated. In contrast to the prototypical mAChR allosteric modulator, heptane 1,7-bis-(dimethyl-3'-phthalimidopropyl)-ammonium bromide (C_7/3-phth), SCH-202676 had no effect on the dissociation kinetics of [^{3}H]N-methylscopolamine ([^{3}H]NMS) at M_1 mAChRs stably expressed in CHO cell membranes. However, SCH-202676 completely inhibited the binding of [^{3}H]NMS in membrane preparations with a Hill slope significantly greater than unity, indicative of positive cooperativity in the binding of the inhibitor. Moreover, SCH-202676 caused dextral shifts of the [^{3}H]NMS saturation binding curve that were greater than expected for a competitive interaction. The addition of C_7/3-phth (100 μM) had no significant effect on the inhibitory potency of SCH-202676. In contrast to the findings in cell membranes, the interaction between SCH-202676 and [^{3}H]NMS in intact M_1 CHO cells yielded saturation and inhibition isotherms that were compatible with the predictions for a competitive interaction. Intact cell assays of acetylcholine-mediated phosphoinositide hydrolysis in the absence or presence of SCH-202676 revealed a mixed competitive/non-competitive mode of interaction that was dependent on the concentration of SCH-202676. These data reveal that the nature of the interaction between SCH-202676 and the M_1 mAChR is dependent on whether it is studied using intact versus broken cell preparations. It is proposed that SCH-202676 utilizes a dual mode of ligand-receptor interaction involving both extra- and intracellular attachment points on the M_1 mAChR that are distinct from the allosteric binding site recognized by prototypical mAChR modulators such as C_7/3-phth.

Ligand binding behavior that deviates from the predictions of simple bimolecular mass action kinetics is invariably classed as either “non-competitive” and/or “allosteric”. Often, these terms are used as empirical descriptors of an unknown mechanism that may or may not reflect a true non-classical mode of drug action. The ability to test whether a drug interacts allosterically at G protein-coupled receptors (GPCRs) is important due to the recognition that many GPCRs contain allosteric binding sites for endogenous and/or synthetic ligands (Christopoulos and Kenakin 2002). These ligands, or allosteric modulators, interact at binding sites on the receptor distinct from that of classic, orthosteric, ligands (agonists and competitive antagonists). However, the manifestations of allosterism are many and varied, and therefore a mechanistic framework is required in order to characterize and quantify the effects of such ligands. The simplest model applied to the study of allosteric interactions at GPCRs is the ternary complex model (TCM), as shown in Figure 1 (Stockton et al. 1983; Ehlert 1988). Upon binding to the allosteric site, ligands that act according to the TCM induce conformational changes at the orthosteric site of the receptor that either enhance or inhibit the binding of an orthosteric ligand; this interaction is reciprocal at equilibrium and leads to positive or negative cooperativity between the two sites on the occupied receptor (Ehlert, 1988; Christopoulos 2002).

One of the best studied model systems for investigation of allosteric ligands has been the muscarinic acetylcholine receptors (mAChRs; Lee and El-Fakahany, 1991; Tucek and Proska, 1995; Ellis, 1997; Christopoulos et al., 1998), and it is currently believed that at least one allosteric site on these receptors is located at a more extracellular level to the orthosteric site (Leppik et al. 1994; Matsui et al. 1995; Christopoulos et al. 1998; Buller et al. 2002). Since the extracellular regions of mAChRs, as well as other GPCRs, tend to show less sequence homology across receptor subtypes than the orthosteric domains, targeting allosteric sites is a logical approach to defining more selective ligands for such GPCRs.

Recently, a novel thiadiazole compound, *N*-(2,3-diphenyl-1,2,4-thiadiazole-5-(2*H*)-ylidene)methanamine (SCH-202676; Figure 2), was identified as an allosteric modulator of a variety of GPCRs including mAChRs (Fawzi et al. 2001). This finding was based on radioligand binding assays performed on membrane preparations derived from cells transfected to individually express different types of GPCRs. In particular, SCH-202676 was found to cause a reduction in both agonist and antagonist maximal binding capacity (B_{max}) with only a slight effect on radioligand affinity when investigated via saturation binding assays at α_2 adrenoceptors. Additional inhibition binding assays also demonstrated an antagonistic effect on the binding of [^{3}H]N-methylscopolamine ([^{3}H]NMS) to M_1 and M_2 mAChRs, although this was not studied in any further detail (Fawzi et al. 2001). Given that the simple TCM (Figure 1) only predicts changes in orthosteric ligand affinity and not B_{max}, the nature of the interaction between SCH-202676 and its target GPCRs is likely to be different from that of classic allosteric modulators that act in accordance with the TCM and/or is different between one GPCR and another.

Therefore, the aim of the present study was to investigate the mode of interaction of SCH-202676 with the M_1 mAChR using radioligand binding and functional assays. For comparative purposes, some experiments used the prototypical and well-characterized mAChR allosteric modulator, heptane, 1,7-bis-(dimethyl-3'-phthalimidopropyl)-ammonium bromide (C_7/3-phth; Figure 2) (Christopoulos et al., 1999). We show that the nature of the interaction between SCH-202676 and the M_1 mAChR is highly dependent on whether it is studied using intact versus broken cell preparations. The non-competitive behaviour of SCH-202676 cannot be explained by the simple TCM and suggests that SCH-202676 may possess a dual mode of ligand-receptor interaction involving both extra- and intracellular attachment points on the M_1 mAChR.

Materials and Methods

Materials

Drugs and chemicals were obtained from the following sources: [^{3}H]*N*-methylscopolamine methyl chloride ([^{3}H]NMS) from NEN Life Science Products, (Boston, MA, USA), [^{3}H]*myo*-inositol from Amersham Pharmacia Biotech (Buckinghamshire, UK), *N*-(2,3-diphenyl-1,2,4-thiadiazole-5-(2*H*)-ylidene)methanamine hydrobromide (SCH-202676) from Tocris Cookson (MO, USA), heptane-1,7-bis-(dimethyl-3´-phthalimidopropyl) ammonium bromide (C_7/3-phth) was synthesized by the Institute of Drug Technology (Boronia, Victoria, Australia), Dulbecco's modified eagle's medium (DMEM) and geneticin from Life Technologies GIBCO BRL (Grand Island, NY, USA), fetal bovine serum was from ThermoTrace, (Melbourne, VIC, Australia), and DOWEX AG1-X8 ion-exchange resin was obtained from Bio-Rad (Hercules, CA, USA). All other materials were obtained from Sigma Chemicals (St. Louis, MO, USA).

Cell culture

Chinese hamster ovary (CHO-K1) cells, stably transfected with the human M_1 mAChR (M_1 CHO cells), were kindly provided by Dr. M. Brann, (University of Vermont Medical School, Burlington, VT). Cells were grown and maintained in DMEM containing 20 mM HEPES, 10% fetal bovine serum and 50 μg/ml geneticin for 4 days at 37°C in a humidified incubator containing 5% CO_2:95% O_2 , before harvesting by trypsinization followed by centrifugation (300 x g, 3 min) and resuspension of the pellet in DMEM.

Cell membrane preparation

M_1 CHO cells were grown, harvested and centrifuged as described above, with the final pellet resuspended in 5 ml of ice-cold Tris-HCl buffer (50 mM Tris, 3 mM $MgCl_2$ and 0.2 mM

EGTA; pH 7.4 with HCl) and then homogenized using a Polytron homogenizer for three 10 s intervals at maximum setting with 30 s cooling periods employed between each burst. The cell homogenate was centrifuged (1,000 x g, 10 min, 25°C), the pellet discarded and the supernatant was re-centrifuged at 30,000 x g for 30 min at 4°C. The resulting pellet containing cell membrane was resupended in 5 ml of Tris-HCl buffer and protein content was determined using the method of Bradford (Bradford 1976). The homogenate was then aliquoted into 1 ml amounts and stored frozen at -80°C until required for radioligand binding assays.

Saturation binding assays

In these assays M_1 CHO cell membranes (10 μg/assay tube) or intact CHO cells (200, 000 cells/ assay tube) were incubated in a total volume of 1 ml HEPES buffer (110 mM NaCl, 5.4 mM KCl, 1.8 mM $CaCl_2$, 1 mM $MgSO_4$, 25 mM glucose, 50 mM HEPES, 58 mM sucrose; pH 7.4) with varying concentrations of [^{3}H]NMS (10 pM to 20 nM) in the absence and presence of different concentrations of SCH-202676 for 1 hr at 37°C. The reaction was then terminated by rapid filtration through Whatman GF/B filters using a Brandell cell harvester. Non-specific binding was determined using 10 μM atropine. Filters were washed three times with 4 ml aliquots of ice-cold saline and dried before radioactivity (dpm) was measured using liquid scintillation counting.

Inhibition binding assays

Initial experiments were performed in a total volume of 1 ml HEPES buffer using M_1 CHO cell membrane homogenates (10 μg/assay tube) or intact cells (100,000 cells/assay tube), incubated with [^{3}H]NMS (0.2 or 2 nM) and various concentrations of SCH-202676 (30 nM to 300 μM) for 1 hr at 37°C, unless otherwise indicated. Additional SCH-202676 experiments

were conducted in M_1 CHO membranes in the presence of 100 μM C_7/3-phth. Non-specific binding, reaction termination and radioactivity determination were as described above.

Radioligand dissociation kinetic assays

[^{3}H]NMS dissociation kinetic binding assays were performed in HEPES buffer, using a reverse time protocol. In these experiments M_1 CHO membranes (10 μg/ assay tube in a total volume of 1 ml) were added to tubes containing [^{3}H]NMS (0.5 nM) in a time-staggered approach so that each replicate was allowed to equilibrate for 1 hr at 37°C. Once the receptors and radioligand had equilibrated, atropine (10 μM) was added at appropriate time intervals to prevent reassociation of [^{3}H]NMS to the M_1 mAChR in the absence or presence of C_7/3-phth or SCH-202676, as indicated in Results. Non-specific binding was determined using atropine (10 μM). In some experiments, SCH-202676 (1 μM) was added alone after [^{3}H]NMS - receptor equilibration in order to prevent re-association of the radioligand. Non-specific binding, reaction termination and radioactivity determination were as described above.

Phosphoinositide (PI) hydrolysis assays

M_1 CHO cells were loaded overnight with [^{3}H]*myo*-inositol (1 μCi/ml) at 37°C in a humidified incubator containing 5% CO_2/95% O_2. On the day of the experiment, cells were harvested and centrifuged (300 x g, 3 min), and the final pellet was re-suspended in 5 ml of HEPES buffer and used for cell counting. The cell suspension was then diluted in HEPES buffer containing 10 mM LiCl, distributed into assay tubes (~ 500,000 cells/tube), and allowed to incubate for 15 min at 37°C. After this pre-incubation period, ACh, SCH-202676 or appropriate vehicle controls (see below) were added to the remaining assay tubes and the reaction was allowed to proceed for a further 30 min before being terminated by stop solution

(methanol:chloroform, 2:1). Assay tubes were centrifuged at 450 x g for 5 min at room temperature, and total inositol phosphates were separated by ion exchange chromatography on Dowex AG1-X8 resin. [^{14}C]inositol-1-phosphate was used as an internal recovery standard. The amount of radioactivity (dpm) in each sample was measured using a liquid scintillation counter and values were corrected for recovery determined for each sample. Initial experiments involved the construction of concentration-response (C-R) curves to increasing concentrations of ACh (10 nM to 1 mM) in the absence or presence of SCH-202676 (1, 10 or 100 μM), which was pre-incubated for 15 min before agonist addition. Further experiments involved the establishment of antagonist inhibition curves using increasing concentrations of SCH-202676 (30 nM to 0.1 mM), in the presence of ACh (1 μM), which was pre-incubated for 15 min before addition of SCH-202676. In these latter experiments a complete C-R curve to ACh was also established in parallel as a measure of the responsiveness of the system to agonist stimulation.

Data analysis

Data sets of total and non-specific binding, derived from each complete saturation binding assay, were analyzed according to the following equation using Prism 4.0 (GraphPad Software, San Diego, CA):

$$\text{Binding} = \frac{B_{max} \cdot [A]}{[A] + K_A} + NS \cdot [A] \qquad (1)$$

where B_{max} denotes the maximal density of binding sites, K_A the radioligand equilibrium dissociation constant and NS the fraction of non-specific binding. The hyperbolic term in equation (1) was not utilized when fitting the non-specific binding data while the parameter,

JPET Fast Forward. Published on November 14, 2003 as DOI: 10.1124/jpet.103.060590
This article has not been copyedited and formatted. The final version may differ from this version.

NS, was shared between both total and non-specific binding datasets. Radioligand inhibition binding isotherms were analyzed according to the following logistic function:

$$Y = \frac{(\text{Top} - \text{Bottom})[I]^{n_H}}{[I]^{n_H} + IC_{50}{}^{n_H}} \qquad (2)$$

where Y denotes the percent specific binding, Top and Bottom denote the maximal and minimal asymptotes, respectively, [I] denotes the inhibitor concentration, IC_{50} denotes the inhibitor potency (midpoint location) parameter and n_H denotes the Hill slope factor. Where appropriate, and assuming simple competition, IC_{50} values were converted to K_I values (inhibitor equilibrium dissociation constant) using the Cheng and Prusoff (1973) equation.

For the dissociation kinetic experiments, complete dissociation curves for the radioligand, in the absence and presence of the highest concentration of applied modulator were evaluated by non-linear regression using the following equation:

$$B_t = B_O \cdot e^{-k_{offobs} \cdot t} \qquad (3)$$

where B_t denotes the specific binding of radioligand at time t, B_0 denotes the specific binding of radioligand at equilibrium (time = 0) and k_{offobs} denotes the observed radioligand dissociation rate constant. For the C_7/3-phth/[^{3}H]NMS dissociation kinetic experiments, datasets were globally fitted to the equation (3) with the parameter, k_{offobs}, defined as follows:

$$k_{offobs} = \frac{[B]^{slope} \cdot \frac{k_{off_B}}{K_B/\alpha} + k_{off}}{1 + \frac{[B]^{slope}}{K_B/\alpha}} \qquad (4)$$

where k_{off} denotes the rate constant for dissociation of the radioligand from the free (unoccupied) receptor, k_{offB} denotes the rate constant for the dissociation of the radioligand from the modulator-occupied receptor, and K_B/α denotes the dissociation constant of the modulator for the radioligand-occupied receptor (Lazareno and Birdsall, 1995; Christopoulos et al. 1999). The parameter, *slope*, denotes an empirical slope factor; a value not significantly different from unity may be taken as presumptive evidence of a simple, one-to-one, mass-action relationship between the allosteric modulator and its binding site on the receptor.

For the functional assays, agonist C-R curves in the absence and presence of antagonist, as well as antagonist inhibition curves, were globally fitted to the following equation using Prism 4 (Motulsky and Christopoulos, 2003):

$$\text{Response}=\frac{(\text{Top-Bottom})}{1+\left(\frac{10^{\text{LogEC}_{50}}\left[1+\left(\frac{[B]}{10^{-pA_2}}\right)^{s}\right]}{[A]}\right)^{n_H}} \qquad (5)$$

where Top represents the maximal asymptote of the C-R curves, Bottom represents the lowest asymptote of the C-R curves, $LogEC_{50}$ represents the logarithm of the agonist EC_{50} in the absence of antagonist, A represents the concentration of the agonist, B represents the concentration of the antagonist, n_H represents the Hill slope of the agonist curve, s represents the Schild slope for the competitive antagonist, and pA_2 represents the negative logarithm of the concentration of antagonist that shifts the agonist EC_{50} by a factor of 2. If the Schild slope was not significantly different from unity, it was constrained as such and the estimate of $-pA_2$ represented the $LogK_B$. Equation 5 was also used to analyze the saturation binding data

obtained using intact cells, with the $LogEC_{50}$ term being replaced by $LogK_A$ and the value of n_H being constrained to 1.

In all cases, potency and affinity values were estimated as logarithms (Christopoulos 1998). Data shown are the mean ± SEM. Comparisons between mean values were performed by unpaired *t* tests. Unless otherwise stated, values of $p < 0.05$ were taken as statistically significant.

Results

Dissociation kinetic assays

A hallmark of many prototypical allosteric modulators of mAChRs is the ability to retard orthosteric ligand dissociation (Kostenis and Mohr, 1996). As shown in Figure 3A, C_7/3-phth produced a concentration-dependent retardation of [^{3}H]NMS dissociation at the M_1 mAChR in CHO cell membranes, indicative of an allosteric mode of action. The dissociation curves for the radioligand in the absence and presence of the highest concentration of modulator were monophasic in all cases, thus, the effects of intermediate concentrations of C_7/3-phth on the apparent radioligand dissociation rate were assessed using a two-point experimental design (Kostenis and Mohr 1996). A constrained simultaneous analysis of each complete family of curves observed per experiment, according to equations 3 and 4, was used to obtain a k_{off} value of 0.31 ± 0.06 min^{-1} (n=3-9) for the dissociation rate of [^{3}H]NMS from the M_1 mAChR in the absence of modulator. The parameter k_{offB} was found to be not significantly different from 0 min^{-1} ($p > 0.05$) and was constrained as such. This finding is consistent with C_7/3-phth being able to completely prevent [^{3}H]NMS dissociation from the receptor. The value for the slope factor in equation 4 was 0.89 ± 0.37 (n=3-9) and found not to differ significantly from unity ($p > 0.05$), implying a simple-mass action relationship between C_7/3-phth and the allosteric binding site. The value of Log(K_B/α) for C_7/3-phth was –5.15 ± 0.08.

In contrast, kinetic assays examining [^{3}H]NMS dissociation in M_1 CHO cell membranes in the absence and presence of SCH-202676 found no effect of the latter compound on radioligand dissociation (Figure 3B). The k_{off} value of 0.29 ± 0.03 min^{-1} (n=4) observed in the presence of 1 μM SCH-202676 was not significantly different ($p > 0.05$) from the control k_{off} value determined in its absence (0.26 ± 0.02 min^{-1}; n=4). Interestingly, the addition of

SCH-202676 alone also resulted in [^{3}H]NMS dissociation (k_{off} of 0.23 ± 0.02 min^{-1}; n=4) that was indistinguishable from that observed in the presence of atropine alone.

Inhibition binding assays using M_1 CHO membranes

In M_1 CHO cell homogenates, SCH-202676 completely inhibited the binding of 0.2 nM [^{3}H]NMS, with a Hill slope (n_H) significantly greater than unity ($p < 0.05$; Figure 4A; Table 1). Increasing the concentration of [^{3}H]NMS from 0.2 to 2 nM did not change the location or shape of the SCH-202676 inhibition curve; the $LogIC_{50}$ value being -6.80 ± 0.09 (n=4) and n_H being 2.52 ± 0.35 in the presence of 2 nM [^{3}H]NMS (Figure 4A).

To investigate whether the steep inhibition curves observed with SCH-202676 were due to possible nonequilibrium artifacts, additional inhibition binding assays utilized a longer equilibration time (2 hr). The $LogIC_{50}$ value of -6.87 ± 0.04 (n=3) obtained for the 2 hr incubation data (not shown) was not significantly different ($p > 0.05$) from that derived from 1 hr equilibration studies.

If SCH-202676 were indeed an allosteric modulator of mAChRs, the dissociation kinetic experiments suggested that it may not mediate its effects via an interaction with the classic allosteric site recognized by C_7/3-phth. To further investigate this hypothesis, inhibition binding assays were repeated with [^{3}H]NMS *versus* SCH-202676 in the absence and presence of C_7/3-phth (100 μM). As shown in Figure 4B, there were no significant changes ($p > 0.05$) in the $LogIC_{50}$ (-6.63 ± 0.08; n = 3) or n_H (2.73 ± 0.49) parameters in the presence of C_7/3-phth when compared to control (Table 1) values, suggesting that SCH-202676 did not share a common site of action with C_7/3-phth.

Saturation binding assays using M_1 CHO membranes

To gain further insight into the possible mechanisms underlying the steep curves observed in the inhibition binding experiments, complete [^{3}H]NMS saturation binding assays were performed. As shown in Figure 5A, a narrow range of concentrations of SCH-202676 caused a profound dextral shift of the radioligand saturation curve such that [^{3}H]NMS occupancy could not be fully determined in the presence of 0.2 and 0.3 μM SCH-202676 (Table 2). In the presence of the lowest concentration of SCH-202676 (0.1 μM), it was noted that there was a significant ($p < 0.05$) shift in the [^{3}H]NMS apparent $LogK_A$ from -9.18 ± 0.06 (n = 4) to -8.68 ± 0.10 (n = 3), but no effect on B_{max}.

Saturation binding assays using M_1 CHO cells

It is possible that the non competitive mode of interaction of SCH-202676 described above reflects its binding to an intracellular domain of the M_1 mAChR that is accessible due to the broken cell nature of the assays. Additional saturation experiments were thus performed using intact M_1 CHO cells, where it was found that SCH-202676 was less potent at inhibiting [^{3}H]NMS saturation binding than in membrane-based experiments (Figure 5B). Importantly, there was no apparent effect of SCH-202676 on the B_{max} of the radioligand, with only the K_A being altered. Assuming a simple competitive mode of interaction, analysis of the data in Figure 5B according to equation 5 yielded a Schild slope of 1.21 ± 0.24, which was not significantly different from unity ($p > 0.05$; F-test). Constraining this value to 1 yielded an estimated $LogK_B$ of -7.23 ± 0.15 for the interaction between SCH-202676 and [^{3}H]NMS in the intact cells.

Inhibition binding assays using M_1 CHO cells

The difference in the binding properties of SCH-202676 at M_1 mAChRs between membranes and intact cells was further illustrated using [^{3}H]NMS inhibition binding assays in intact cells.

Figure 6 and Table 1 show that the inhibition binding curve for SCH-202676 was significantly shallower in intact cells compared to membranes. Because the Hill slope obtained from SCH-202676 binding in the intact cells were not significantly different to 1 ($p > 0.05$; F-test) the IC_{50} value was converted to a K_I value, yielding a $LogK_I$ estimate for the interaction between SCH-202676 and [^{3}H]NMS of -6.71 ± 0.14 (n=4) in intact cells. This value was not significantly different ($p > 0.05$) from the $LogK_B$ value determined above from the intact cell saturation binding assays.

PI hydrolysis assays

To determine the effects of SCH-202676 on cellular function, PI hydrolysis experiments were conducted in intact M_1 CHO cells under similar assay conditions to those used in the radioligand binding experiments. As shown in Figure 7, ACh was able to mediate a robust response in PI accumulation. In contrast, SCH-202676 alone (up to 100 μM) had no effect on basal PI hydrolysis (data not shown). The presence of increasing concentrations of SCH-202676 led to progressive dextral displacements of the ACh C-R curves (Figure 7A). Although no significant effect was noted on the maximal agonist response in the presence of 1 μM SCH-202676, as expected for a competitive interaction, higher concentrations caused a significant reduction in ACh E_{max} values ($p < 0.05$; Figure 7A, Table 2). Without prejudice to mechanism, the shift of the ACh concentration-response curve observed in the presence of 1 μM SCH-202676 was used to derive an apparent $LogK_B$ value against ACh, which was -6.27 ± 0.23 (n = 5).

To examine a larger range of SCH-202676 concentrations on ACh function, antagonist inhibition curves were constructed against the response to a fixed (1 μM) concentration of ACh (Figure 7B). Analysis of the data using equation 5 gave a Schild slope of 0.95 ± 0.08 (n=3), which was not significantly different from unity using an F test ($p > 0.05$).

Constraining the Schild slope to 1 yielded a $\log K_B$ value of -6.28 ± 0.15 (n=3).

JPET Fast Forward. Published on November 14, 2003 as DOI: 10.1124/jpet.103.060590
This article has not been copyedited and formatted. The final version may differ from this version.

Discussion

The development of selective allosteric compounds is currently of great therapeutic relevance, especially in the field of GPCRs (Christopoulos 2002). The present study used the M_1 mAChR to investigate the pharmacology of a recently identified GPCR allosteric ligand. Although some of the findings reported herein confirm and extend a previous (and thus far the only) report of the effect of SCH-202676 as a non-competitive inhibitor of GPCR binding and function (Fawzi et al., 2001), they also highlight striking differences in the pharmacological properties of the compound when studied in intact cells compared to broken-cell preparations. SCH-202676 may possess a dual mode of interaction at the M_1 mAChR that utilizes both extracellular and intracellular receptor attachment points. Furthermore, the interaction of this compound with the M_1 mAChR does not appear to involve the well-defined allosteric site recognized by more specific mAChR modulator ligands, such as C_7/3-phth.

A key theoretical advantage of allosteric modulators of GPCRs that act according to the TCM (Figure 1) is the potential for greater selectivity of action. This can arise due to modulator specificity for receptor binding domains that are not conserved across receptor subtypes, and/or due to differential degrees of cooperativity between orthosteric and allosteric sites at a particular receptor subtype compared to others (Lazareno at al, 1998; Birdsall et al., 1999; Christopoulos and Kenakin, 2002). Although SCH-202676 possesses the desirable property of being a synthetic small molecule ligand, there are a number of experimental observations to suggest that it does not act according to the TCM. First, unlike C_7/3-phth, which is a prototypical mAChR modulator (Christopoulos and Mitchelson, 1994; Lanzafame et al., 1996; Christopoulos et al., 1999), SCH-202676 does not promote a change in receptor conformation that manifests as an alteration in orthosteric radioligand dissociation (Figure 3). Second, membrane-based inhibition binding assays between SCH-202676 and [^{3}H]NMS were

characterized by Hill slopes significantly greater than unity (Figure 4, Table 1), which is not predicted by the simple TCM and not observed with C_7/3-phth under similar assay conditions (Christopoulos and Mitchelson, 1998; Christopoulos et al, 1999). Third, the TCM predicts that negative allosteric modulators can display a progressive inability to fully inhibit specific radioligand binding when the concentration of the radioligand is increased (Christopoulos and Kenakin, 2002); increasing the concentration of [^{3}H]NMS by a factor of 10 had no effect whatsoever on the shape or location of the SCH-202676 inhibition curve (Figure 4A), in contrast to previous observations with C_7/3-phth (Christopoulos and Mitchelson, 1998; Christopoulos et al., 1999). Finally, the inhibition binding isotherm for SCH-202676 was not significantly modified by the addition of C_7/3-phth (Figure 4B), indicating that these two ligands do not compete for the same topographically distinct binding domain on the mAChR.

Another aspect of the pharmacology of SCH-202676 that is not in accord with the TCM was reported by Fawzi et al. (2001) during studies of agonist and antagonist binding to α_2 adrenoceptors, namely, a significant inhibition by SCH-202676 of radioligand B_{max} values with only a minimal effect on radioligand affinity. In the present study, similar membrane-based binding experiments at the M_1 mAChR using [^{3}H]NMS in the presence of increasing concentrations of SCH-202676 revealed a different pattern of behavior, that is, a marked change in apparent radioligand affinity with no clear effect on radioligand B_{max} (Figure 5A). Unfortunately, these experiments were limited by the lack of concentrations of [^{3}H]NMS large enough to define full radioligand-receptor occupancy in the presence of all concentrations of SCH-202676 that were tested. Nevertheless, it is clear that the apparent shifts of the [^{3}H]NMS saturation curves are much greater than expected for simple competition, and may be indicative of positive cooperativity in the binding of SCH-202676 to the M_1 mAChR. This type of cooperative interaction would also be expected to yield steep radioligand inhibition curves, as was indeed observed in this study (Figure 4).

Given the possibility of cooperativity in the binding of SCH-202676, and the previous suggestion by Fawzi et al. (2001) that the compound may be utilizing an intracellular attachment point conserved across different GPCRs, subsequent experiments in our study focused on the pharmacology of the modulator in intact cells. In addition to being more physiologically relevant than membrane-based studies, it was anticipated that the intact cell assays would provide further insight into the mode of action of SCH-202676 at the M_1 mAChR. Significant differences were indeed noted for the interaction between SCH-202676 and [^{3}H]NMS in whole CHO cells compared to homogenates; both intact cell saturation and inhibition assays yielded binding curves that were in accord with the predictions of simple competitive antagonism, such as parallel dextral shifts of the [^{3}H]NMS saturation curve with no change in B_{max} (Figure 5B) and a Hill slope factor not significantly different from unity (Figure 6; Table 1). The assumption of a competitive interaction in the intact cell binding studies allowed for the estimation of apparent SCH-202676 $LogK_B$ values that were not significantly different from one another. This finding suggests that, in intact cells, SCH-202676 may not readily access the intracellular milieu but, rather, bind to an extracellular attachment point on the mAChR and interact in a pseudo-competitive manner with orthosteric ligands such as [^{3}H]NMS.

The ability of SCH-202676 to antagonize ACh-mediated PI hydrolysis (Figure 7) is also in agreement with the finding by Fawzi et al. (2001) that the inhibitory effects of SCH-202676 extend to GPCR agonists, as well as antagonists. Importantly, the assay used in the present study utilized intact CHO cells, in contrast to the membrane-based [^{35}S]GTPγS functional studies of Fawzi et al. (2001). The observation that concentrations of SCH-202676 less than 10 μM appear to interact competitively with ACh supports the findings in the intact cell binding assays. However, higher concentrations of the modulator resulted in a profound

inhibition of the maximal attainable agonist effect. There are at least four possibilities to account for this effect of SCH-202676. The first is that the apparent non-competitive inhibition of ACh-mediated responses at the highest concentrations of SCH-202676 reflect a non-specific, toxic effect. Although we cannot totally rule out this possibility, we deem it unlikely as SCH-202676 alone (up to 100 μM) had no effect on basal (receptor-independent) PI hydrolysis. The second possibility is that, in intact cells, SCH-202676 binds in a pseudo-irreversible manner to the orthosteric site on the M_1 mAChR, and that the progressive decline in ACh maximal responsiveness represents the progressive diminution of receptor reserve by increasing concentrations of SCH-202676. However, this is also unlikely because binding assays using prolonged equilibration times found no evidence for an enhanced antagonistic effect of SCH-202676, and Fawzi et al. (2001) have previously demonstrated that the compound can be washed out after prolonged exposure to cell membranes. The third possibility is that the effects of SCH-202676 are purely non-competitive and mediated entirely via an allosteric site on the M_1 mAChR that is topographically distinct from the better-characterized allosteric site recognized by modulators such as C_7/3-phth. Although possible, this cannot account for the markedly different effects of the inhibitor when assayed in membranes compared to intact cells if the same allosteric site mediates the inhibition in each instance. A final possibility is that SCH-202676 recognizes more than one site on the mAChR, with an extracellular attachment point that preferentially mediates the effects seen in intact cells, and an intracellular attachment point that contributes to the effects seen in membranes; the non-competitive inhibition of agonist function noted with high micromolar concentrations of SCH-202676 may then represent a concentration gradient-driven accumulation of some of the compound in the proximity of or at the intracellular attachment point. This dual binding-mode mechanism can also account for the apparent cooperativity in binding noted for SCH-202676 in the membrane assays, where, presumably, both attachment points on the receptor are readily accessible to the modulator.

Irrespective of the mechanism of action of SCH-202676, the current findings highlight important issues in the study of allosteric modulators of GPCRs. For instance, as suggested by Fawzi et al. (2001) and supported by some of the findings of the present study, SCH-202676 may recognize a conserved regulatory domain that is located in the intracellular-facing regions of the receptor. In terms of drug discovery, such a site is a relatively unattractive target for two reasons. First, intracellular targets are generally not as readily accessible as extracellular targets, and antagonizing intracellular GPCR domains may impair receptor coupling to accessory cellular proteins in addition to modulating ligand binding. Second, the conserved nature of such a regulatory site implies that ligands acting at this site will lack receptor specificity; allosteric modulators that target less conserved domains on GPCRs are preferable therapeutic candidates. Another important issue highlighted by the present study is that the nature of the assay (e.g., broken cell *versus* intact cell) can reveal marked differences in the apparent mode of action of modulator ligands. Given that SCH-202676 represents a useful small molecule tool with which to study certain aspects of GPCR allosteric modulation, it would be interesting to determine whether it displays more than one possible mode of interaction at other GPCRs.

Acknoweldgements

The authors would like to thank Ms Elizabeth Guida for expert technical assistance. We are also grateful to Drs Patrick Sexton and Fred Mitchelson for critical review of the manuscript.

References

Birdsall N. J., Farries T., Gharagozloo P., Kobayashi S., Lazareno S. and Sugimoto M. (1999) Subtype-selective positive cooperative interactions between brucine analogs and acetylcholine at muscarinic receptors: functional studies. *Mol Pharmacol* **55:** 778-786.

Bradford M. M. (1976) A rapid and sensitive method for the quantitation of microgram quantities of protein utilizing the principle of protein-dye binding. *Anal. Biochem.* **72:** 248-254.

Buller S., Zlotos D. P., Mohr K. and Ellis J. (2002) Allosteric site on muscarinic acetylcholine receptors: a single amino acid in transmembrane region 7 is critical to the subtype selectivities of caracurine V derivatives and alkane-bisammonium ligands. *Mol Pharmacol* **61:** 160-168.

Cheng Y-C and Prusoff WH (1973) Relationship between the inhibition constant (K_I) and the concentration of inhibitor which causes 50 per cent inhibition (I_{50}) of an enzymatic reaction. *Biochem. Pharmacol.* **22**: 3099-3108.

Christopoulos A. (2002) Allosteric binding sites on cell-surface receptors: novel targets for drug discovery. *Nat Rev Drug Discov* **1:** 198-210.

Christopoulos A. and Kenakin T. (2002) G protein-coupled receptor allosterism and complexing. *Pharmacol Rev* **54:** 323-374.

Christopoulos A. (1998) Assessing the distribution of parameters in models of ligand-receptor interaction: to log or not to log. *Trends Pharmacol. Sci.* **19:** 351-357.

Christopoulos A and Mitchelson F (1998) Use of a spreadsheet to quantitate the equilibrium binding of an allosteric modulator. *Eur J Pharmacol* **355**: 103-111.

Christopoulos A., Lanzafame A. and Mitchelson F. (1998) Allosteric interactions at muscarinic cholinoceptors. *Clin Exp Pharmacol Physiol* **25:** 185-194.

Christopoulos A and Mitchelson F (1994) Assessment of the allosteric interactions of the bisquaternary heptane-1,7-bis(dimethyl-3'-pthalimidopropyl)ammonium bromide at M_1 and M_2 muscarine receptors. *Mol Pharmacol* **46**: 105-114.

Christopoulos A., Sorman J. L., Mitchelson F. and El-Fakahany E. E. (1999) Characterization of the subtype selectivity of the allosteric modulator heptane-1,7-bis-(dimethyl-3'-phthalimidopropyl) ammonium bromide (C_7/3-phth) at cloned muscarinic acetylcholine receptors. *Biochem Pharmacol* **57:** 171-179.

Ehlert F. J. (1988) Estimation of the affinities of allosteric ligands using radioligand binding and pharmacological null methods. *Mol Pharmacol* **33:** 187-194.

Ellis J (1997) Allosteric binding sites on muscarinic receptors. *Drug Dev. Res.* **40**: 193-204.

Fawzi A. B., Macdonald D., Benbow L. L., Smith-Torhan A., Zhang H., Weig B. C., Ho G., Tulshian D., Linder M. E. and Graziano M. P. (2001) SCH-202676: An allosteric modulator of both agonist and antagonist binding to G protein-coupled receptors. *Mol Pharmacol* **59:** 30-37.

Kostenis E. and Mohr K. (1996) Two-point kinetic experiments to quantify allosteric effects on radioligand dissociation. *Trends Pharmacol Sci* **17:** 280-283.

Lanzafame A, Christopoulos A and Mitchelson F (1996) Interactions of agonists with an allosteric antagonist at muscarinic acetylcholine M_2 receptors. *Eur J Pharmacol* **316**: 27-32.

Lazareno S. and Birdsall N. J. (1995) Detection, quantitation, and verification of allosteric interactions of agents with labeled and unlabeled ligands at G protein-coupled receptors:

interactions of strychnine and acetylcholine at muscarinic receptors. *Mol Pharmacol* **48:** 362-378.

Lazareno S, Gharagozloo P, Kuonen D, Popham A and Birdsall NJM (1998) Subtype-selective positive cooperative interactions between brucine analogues and acetylcholine at muscarinic recptors: Radioligand binding studies. *Mol Pharmacol* **53**: 573-589.

Lee NH and El-Fakahany EE (1991) Allosteric antagonists of the muscarinic acetylcholine receptor. *Biochem Pharmacol* **42**, 199-205.

Leppik R. A., Miller R. C., Eck M. and Paquet J. L. (1994) Role of acidic amino acids in the allosteric modulation by gallamine of antagonist binding at the m2 muscarinic acetylcholine receptor. *Mol Pharmacol* **45:** 983-990.

Matsui H., Lazareno S. and Birdsall N. J. (1995) Probing of the location of the allosteric site on m1 muscarinic receptors by site-directed mutagenesis. *Mol Pharmacol* **47:** 88-98.

Motulsky H. J. and A. Christopoulos (2003) Fitting models to biological data using linear and nonlinear regression. GraphPad Software, San Diego, CA, USA.

Stockton J. M., Birdsall N. J., Burgen A. S. and Hulme E. C. (1983) Modification of the binding properties of muscarinic receptors by gallamine. *Mol Pharmacol* **23:** 551-557.

Tucek S and Proska J (1995) Allosteric modulation of muscarinic acetylcholine receptors. *Trends Pharmacol Sci* **16:** 205-212.

Footnote

This work was supported by Grant No. 251538 of the National Health and Medical Research Council (NHMRC) of Australia. Arthur Christopoulos is a Senior Research Fellow of the NHMRC. Alfred Lanzafame is the recipient of a NHMRC Dora Lush Biomedical Postgraduate Scholarship.

Address for reprints

Dr. Arthur Christopoulos, NHMRC Senior Research Fellow, Department of Pharmacology, University of Melbourne, Grattan St., Parkville, 3010, Victoria, Australia; Ph: +613 8344 8417; Fax: +613 8344 0241; email: arthurc1@unimelb.edu.au

Figure Legends

Figure 1 The ternary complex model, where A represents orthosteric ligand, B represents allosteric ligand, K_A and K_B represent equilibrium dissociation constants for the binding of ligands A and B respectively, α represents the cooperativity factor for the allosteric interaction between ligand B and ligand A. In this model $\alpha > 1$ denotes positive cooperativity, $\alpha < 1$ denotes negative cooperativity and $\alpha = 1$ denotes neutral cooperativity.

Figure 2 Structures of SCH-202676 and C_7/3-phth.

Figure 3 Effects of (A) C_7/3-phth or (B) SCH-202676 on the dissociation of [^{3}H]NMS in CHO cell membranes expressing the M_1 mAChR. Membranes were equilibrated with 0.5 nM [^{3}H]NMS at 37°C for 1 hr in HEPES buffer after which reassociation was prevented by the addition of 10 μM atropine alone (■) or in combination with 10 μM (▼), 30 μM(◆), 100 μM(▲) or 300 μM (●) C_7/3-phth (Panel A) or 1 μM SCH-202676 (◇) (Panel B). Additional experiments were also performed where radioligand dissociation was monitored after the addition of 1 μM SCH-202676 alone (○) (Panel B). Data points represent the mean ± SEM of 3-9 experiments conducted in triplicate. Where error bars are not shown they lie within the dimensions of the symbol.

Figure 4 Inhibition binding of SCH-202676 (closed symbols), or DMSO vehicle equivalents (open symbols) against: 0.2 nM (■) or 2 nM (●) [^{3}H]NMS (Panel A); or against 0.2 nM [^{3}H]NMS in the absence (■) and presence (●) of 100 μM C_7/3-phth (Panel B) at human M_1 mAChRs expressed in CHO cell membranes. Incubation was for 1 hr at 37°C in HEPES buffer, pH 7.4. Non-specific binding was defined by 10 μM atropine. Data points

represent the mean ± SEM of 3-4 experiments conducted in duplicate. Where error bars are not shown they lie within the dimensions of the symbol.

Figure 5 (A) Normalized saturation binding of [^{3}H]NMS in the absence (■; B_{max} = 5466 ± 696 fmol/mg protein) and presence of 0.1 μM (□), 0.2 μM (○), or 0.3 μM (◇) SCH-202676 at human M_1 mAChRs expressed in CHO cell membranes. Dashed lines were generated assuming no change in the maximal asymptote, to illustrate the profound dextral shift that may be mediated by SCH-202676. Data points represent the mean ± SEM of 3-9 experiments conducted in duplicate. (B) Normalized saturation binding of [^{3}H]NMS in the absence (■; B_{max} = 71 ± 17 fmol/10^5 cells) and presence of 0.1 μM (□), 0.2 μM (○), or 1 μM (△) SCH-202676 at human M_1 mAChRs expressed in intact CHO cells. Data points represent the mean ± SEM of 3-4 experiments conducted in duplicate. Where error bars are not shown they lie within the dimensions of the symbol. Curves through the datapoints represent the best global fit of a competitive binding model (Equation 5 in the Methods) to all datasets.

Figure 6 Inhibition binding of SCH-202676 (closed symbols), or DMSO vehicle equivalents (open symbols) against 0.2 nM [^{3}H]NMS at human M_1 mAChRs expressed in CHO cell membranes (●) or intact CHO cells (■). Data points represent the mean ± SEM of 3-4 experiments conducted in duplicate. Where error bars are not shown they lie within the dimensions of the symbol.

Figure 7 Effects of SCH-202676 on ACh-mediated PI hydrolysis in M_1 CHO cells. (A) Normalized ACh concentration-response curves in the absence (■; E_{max} = 36,000 ± 5800 d.p.m.) and presence of 1 μM (▽), 10 μM (□) or 100 μM (○) SCH-202676 in M_1 CHO

cells. Cells were equilibrated with SCH-202676 for 15 min at 37°C before the addition of ACh for a further 30 min in HEPES buffer. Data points represent the mean ± SEM of 3-11 experiments conducted in triplicate. Where error bars are not shown they lie within the dimensions of the symbol. (B) Concentration-response curve for ACh-mediated PI hydrolysis (■) and antagonist inhibition curve for SCH-202676 in the presence of 1 μM ACh (●). Cells were equilibrated with a fixed concentration of SCH-202676 or ACh for 15 min at 37°C before the addition of a range of concentrations of ACh or SCH-202676, respectively, for a further 30 min in HEPES buffer. Data points represent the mean ± SEM of 3 experiments conducted in triplicate. Where error bars are not shown they lie within the dimensions of the symbol.

JPET Fast Forward. Published on November 14, 2003 as DOI: 10.1124/jpet.103.060590
This article has not been copyedited and formatted. The final version may differ from this version.

Table 1 Inhibition binding parameters for SCH-202676 against 0.2nM [^{3}H]NMS at M_1 mAChRs expressed in CHO cell membranes *versus* intact CHO cells, determined using an equilibrium binding assay.

Parameter	Membranes	Intact cells
$LogIC_{50}$[a]	-6.78 ± 0.04	-6.54 ± 0.13
n_H[b]	2.58 ± 0.25*****	1.06 ± 0.04*****

[a] Logarithm of the midpoint potency parameter for SCH-202676 (n=4-6)

[b] Hill slope factor

***** Student's t test found a significant ($p < 0.05$) difference between experiments using membranes *versus* intact cells.

JPET Fast Forward. Published on November 14, 2003 as DOI: 10.1124/jpet.103.060590
This article has not been copyedited and formatted. The final version may differ from this version.

Table 2 Concentration-response curve parameters for ACh in the absence and presence of SCH-202676 at M_1 mAChRs expressed in CHO cells, determined using a functional PI hydrolysis assay. Values are the mean ± SEM of 3-11 experiments conducted in triplicate.

Parameters[a]	**SCH-202676 (μM)**			
	0	**1**	**10**	**100**
$\mathbf{E_{max}}^{a}$	100 ± 1	100 ± 5	78 ± 5*	1.7 ± 0.1*
$\mathbf{LogEC_{50}}^{b}$	-6.78 ± 0.06	-6.34 ± 0.05*	-5.66 ± 0.09*	-
$\mathbf{n_H}^{c}$	1.79 ± 0.15	1.61 ± 0.09	1.42 ± 0.06	1.31 ± 0.49

[a] Maximum effect is expressed as percentage of the vehicle-treated ACh maximum response.

[b] Logarithm of the EC_{50}.

[c] Hill slope factor.

* Student's t test found a significant ($p < 0.05$) difference between control and SCH-202676-treated groups.

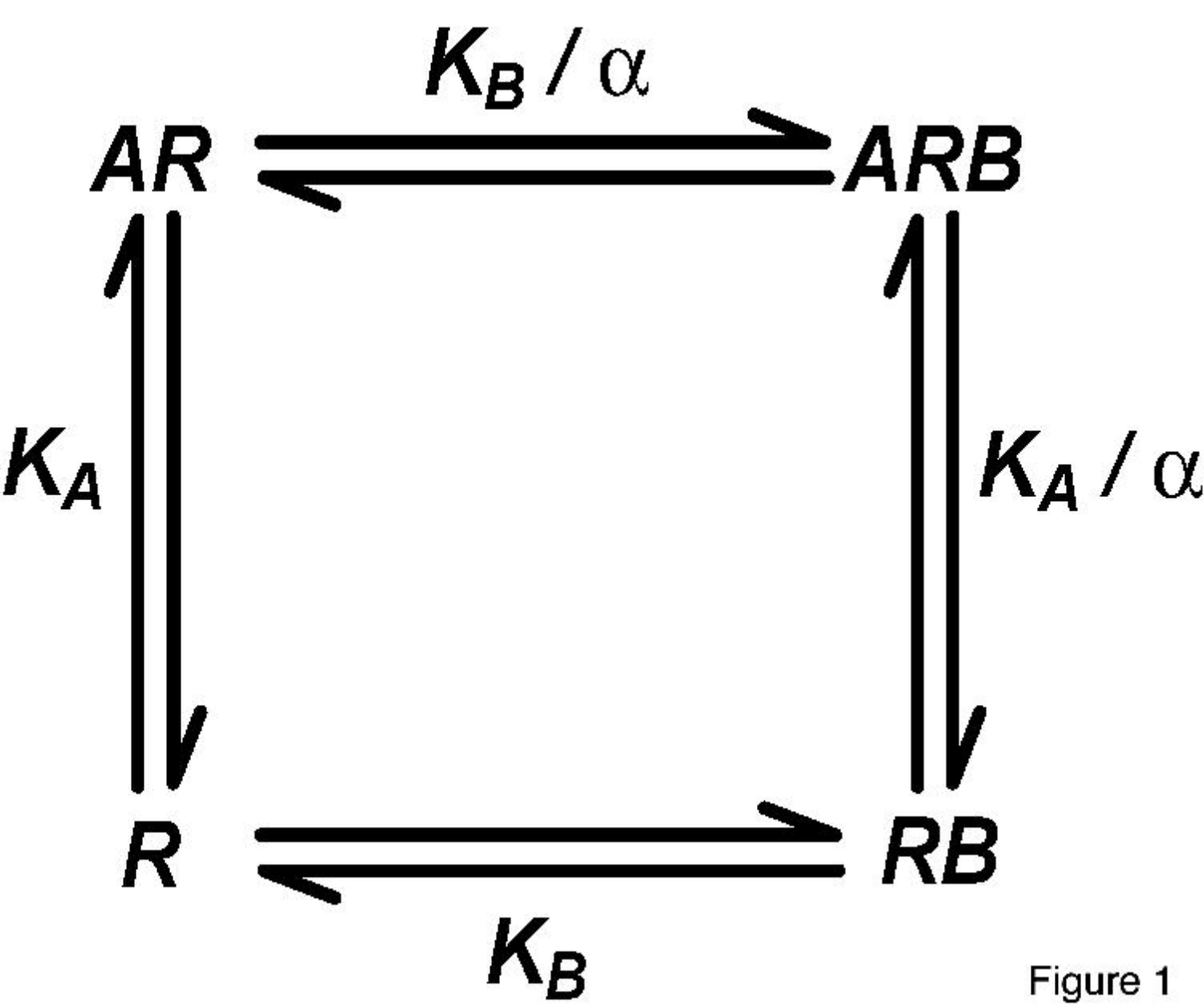

Figure 1

Figure 2

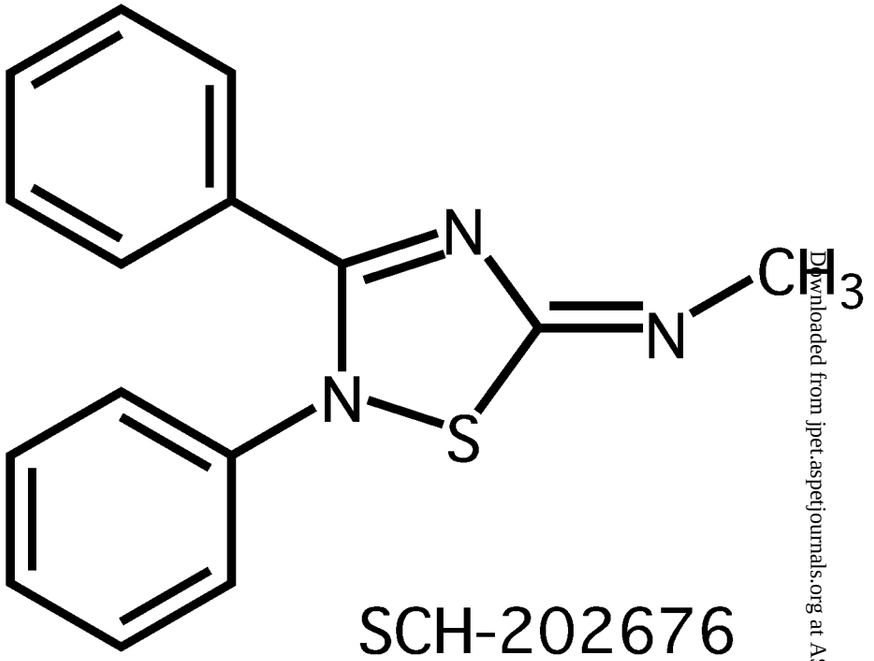

SCH-202676

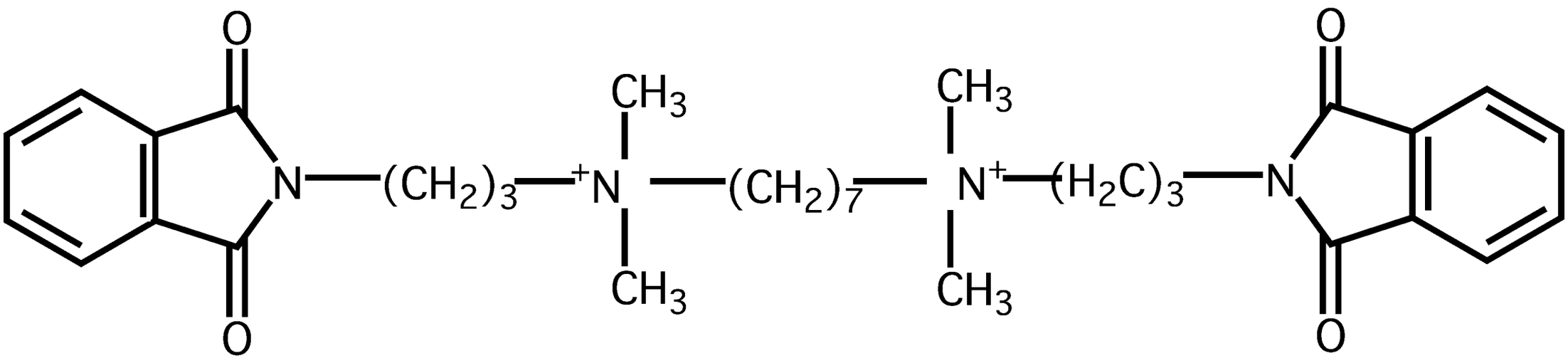

C_7/3-phth

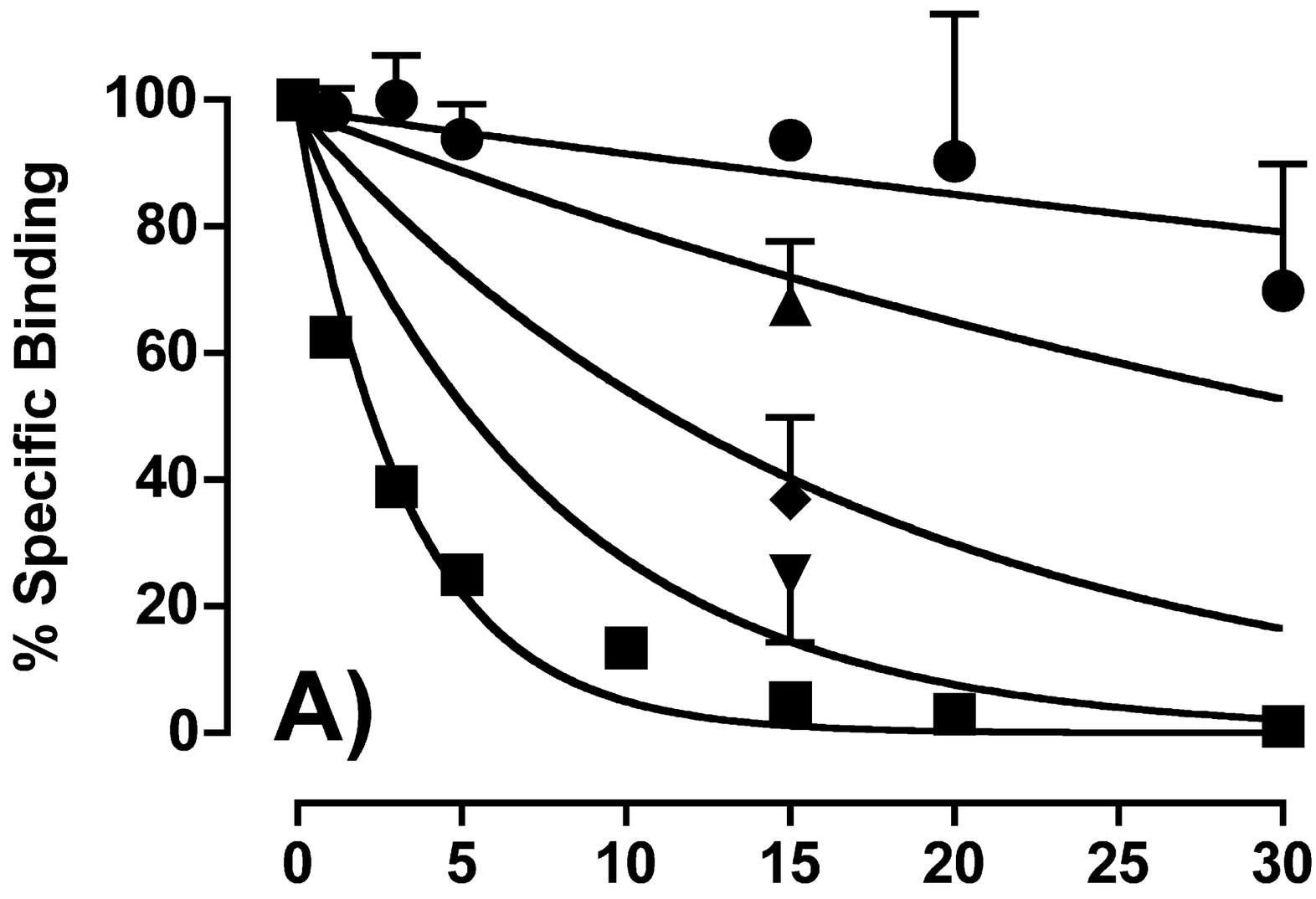

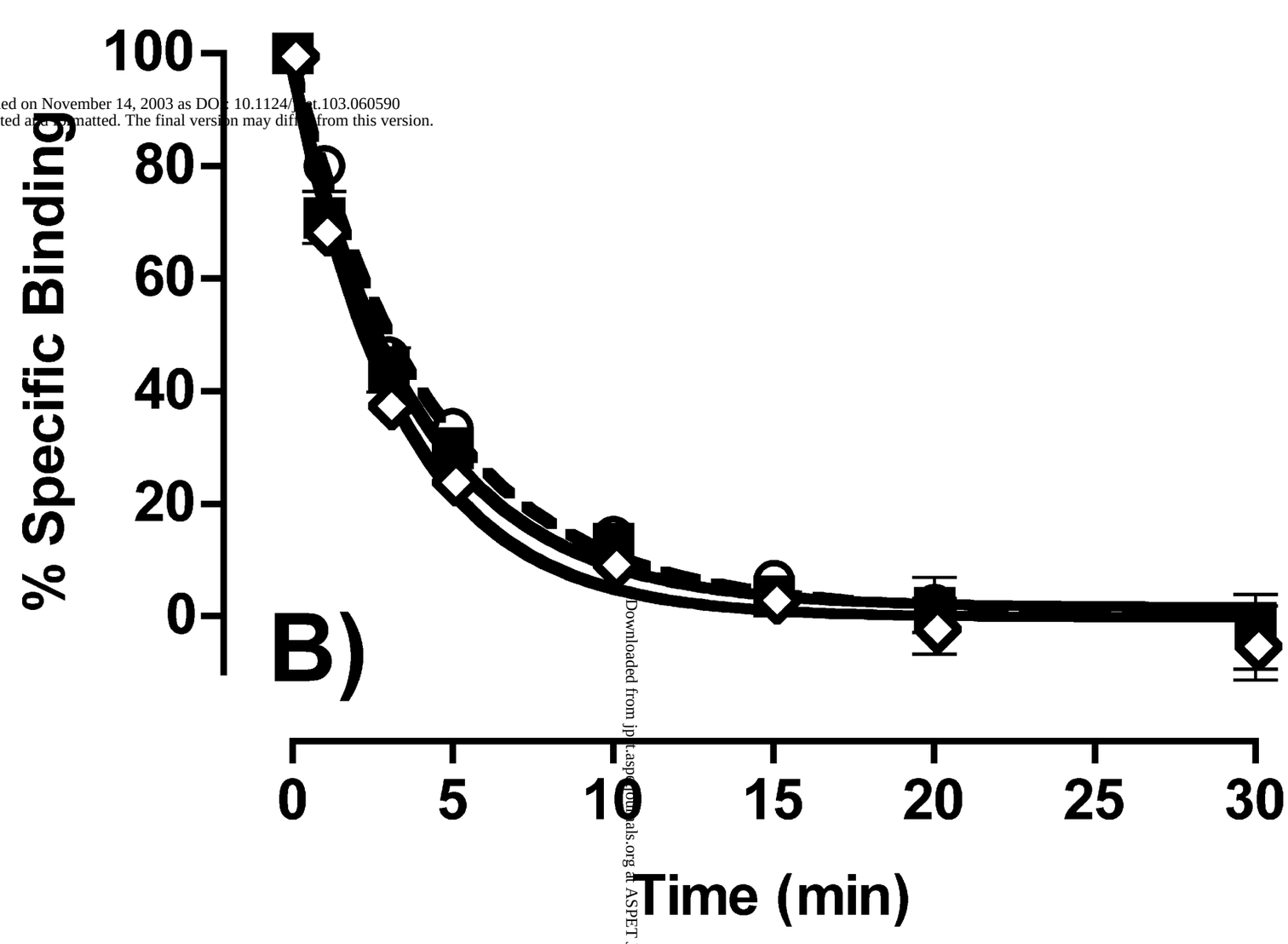

Figure 3

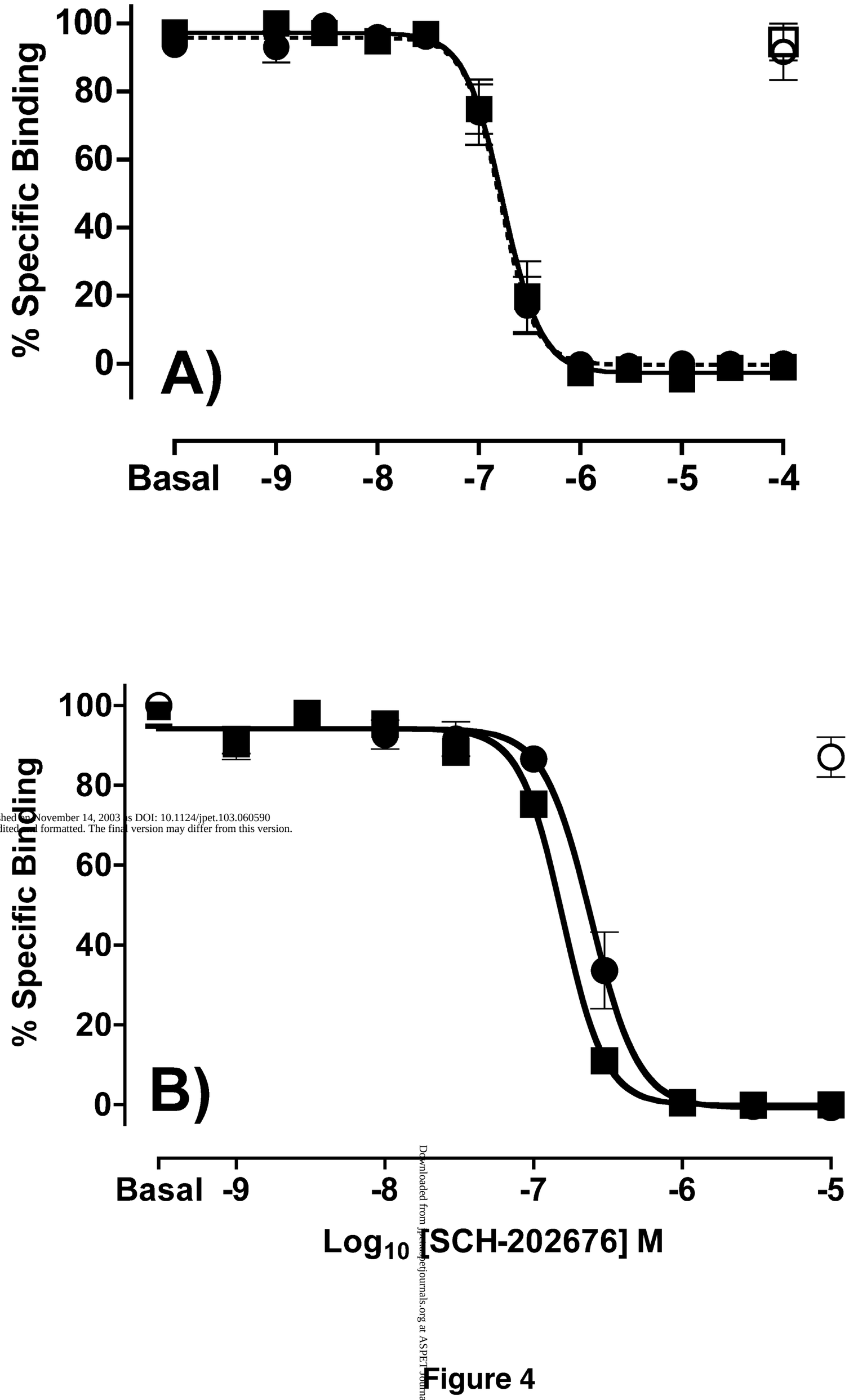

JPET Fast Forward. Published on November 14, 2003 as DOI: 10.1124/jpet.103.060590
This article has not been copyedited and formatted. The final version may differ from this version.

Figure 4

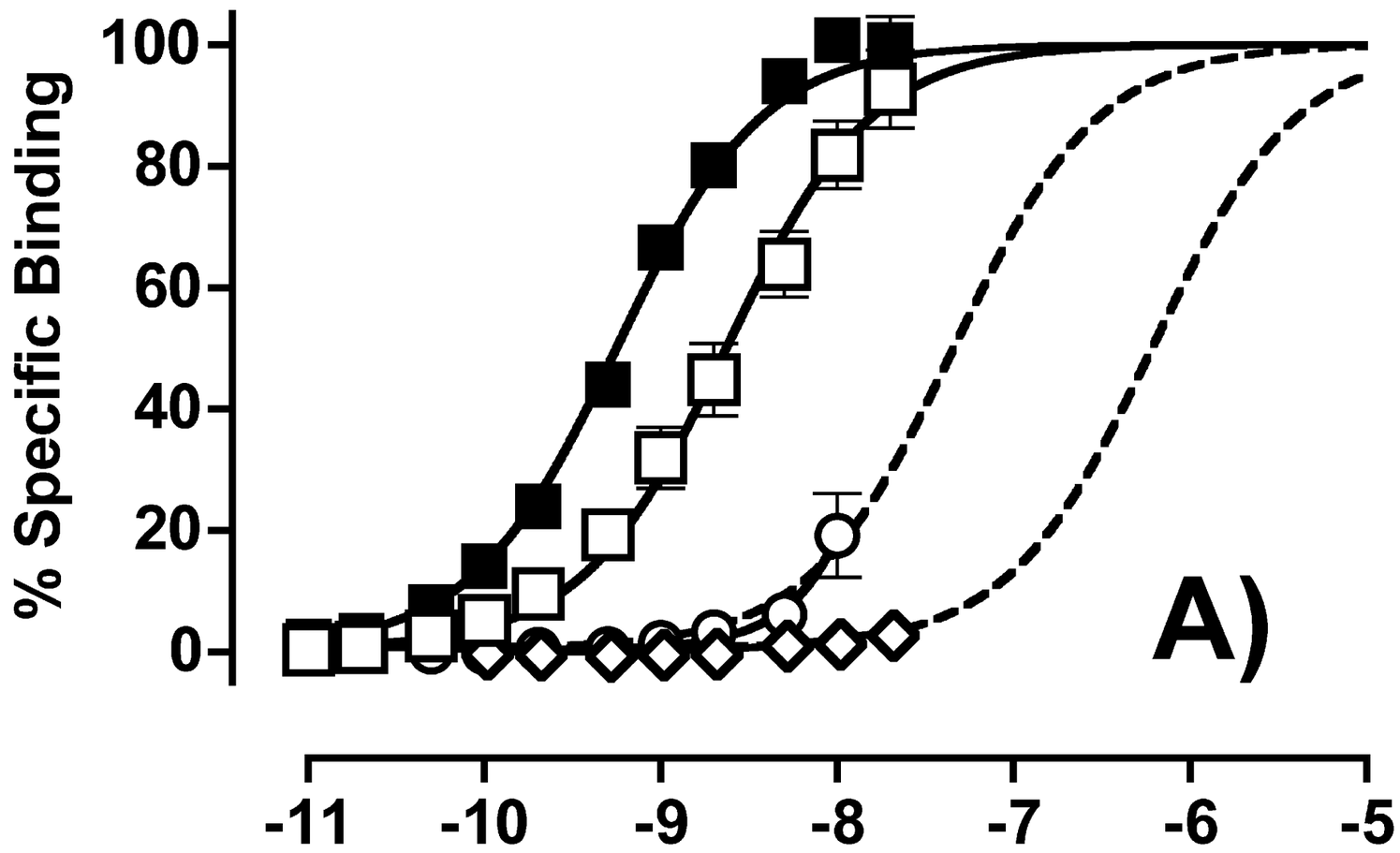

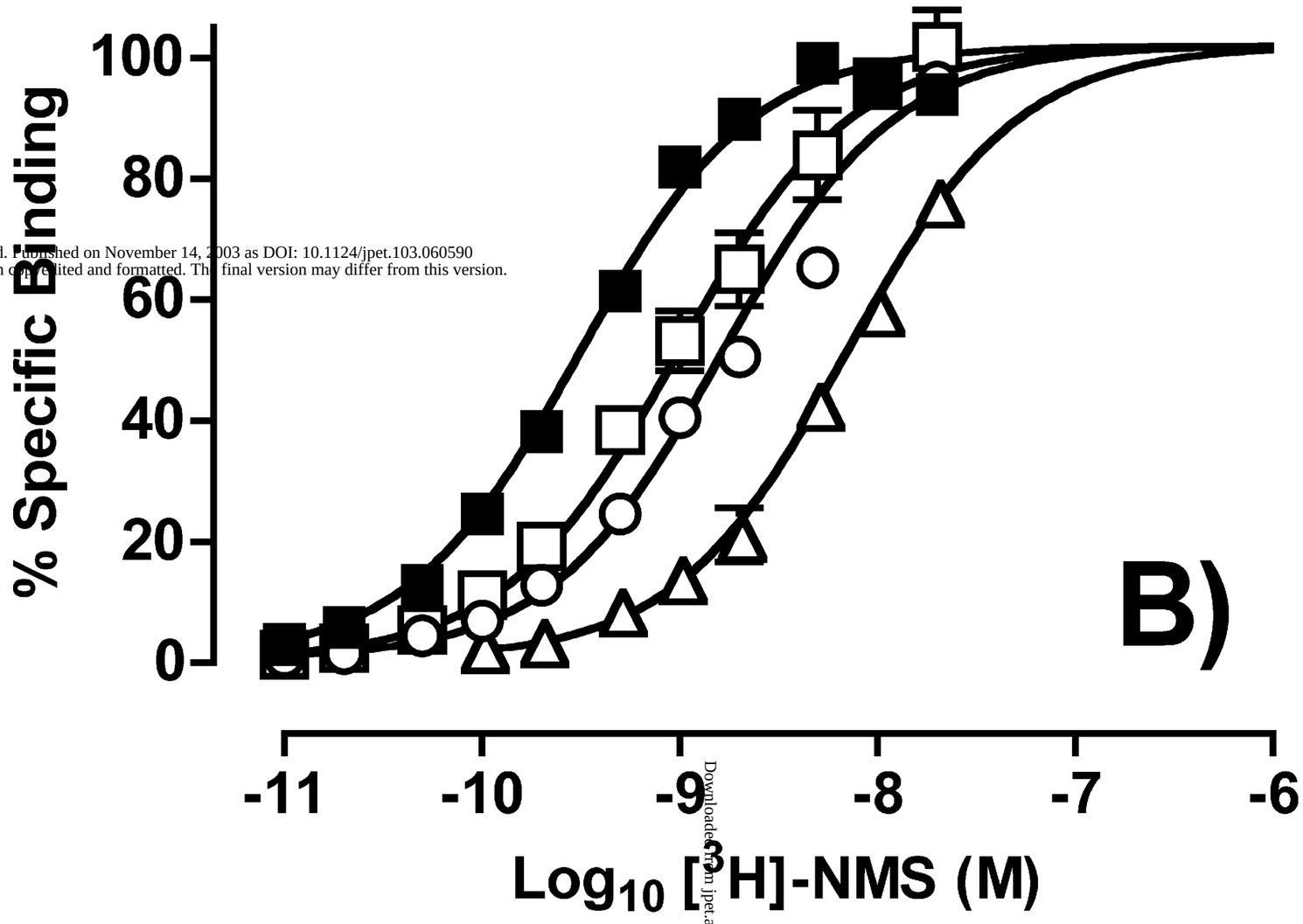

Figure 5

Figure 6

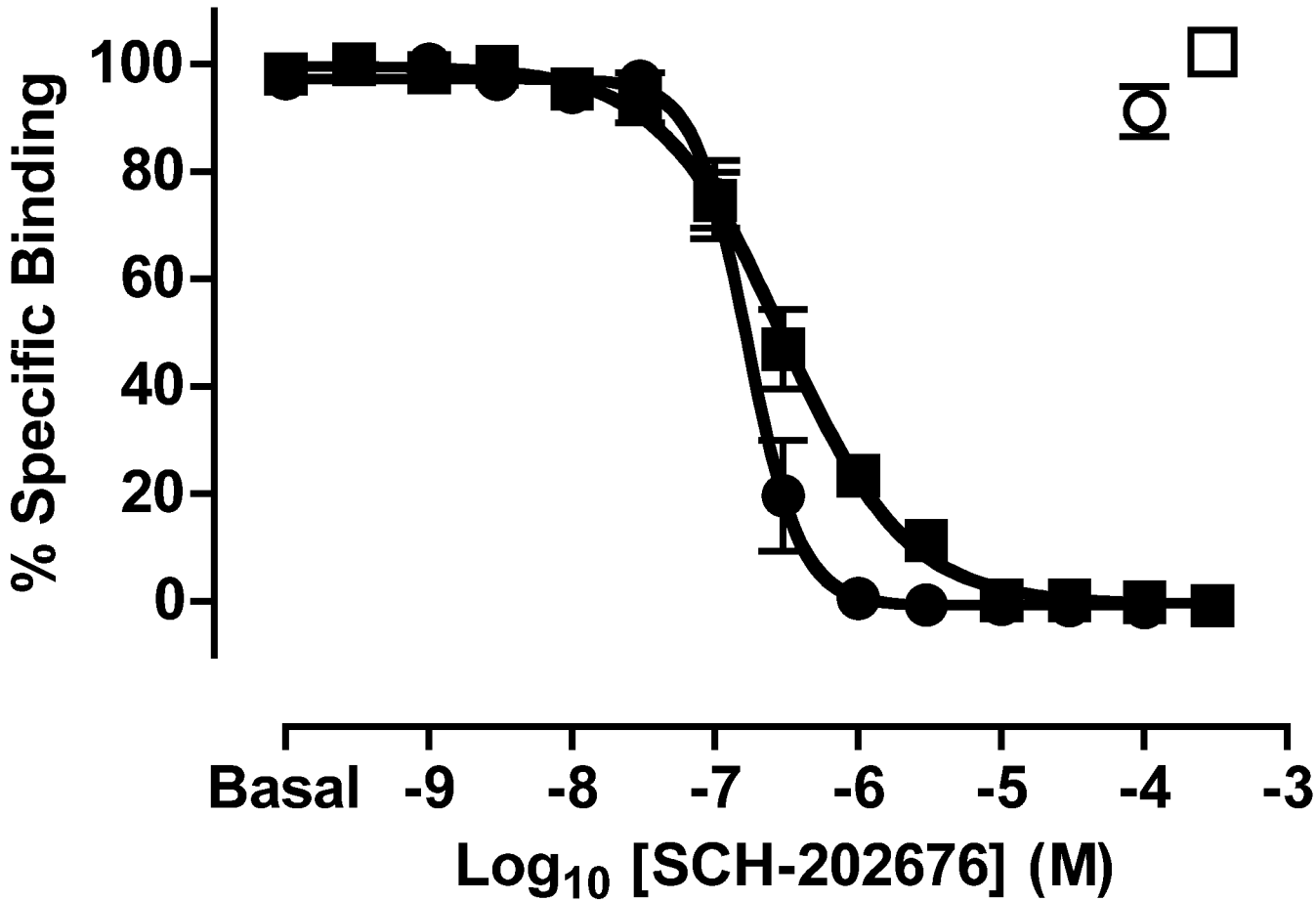

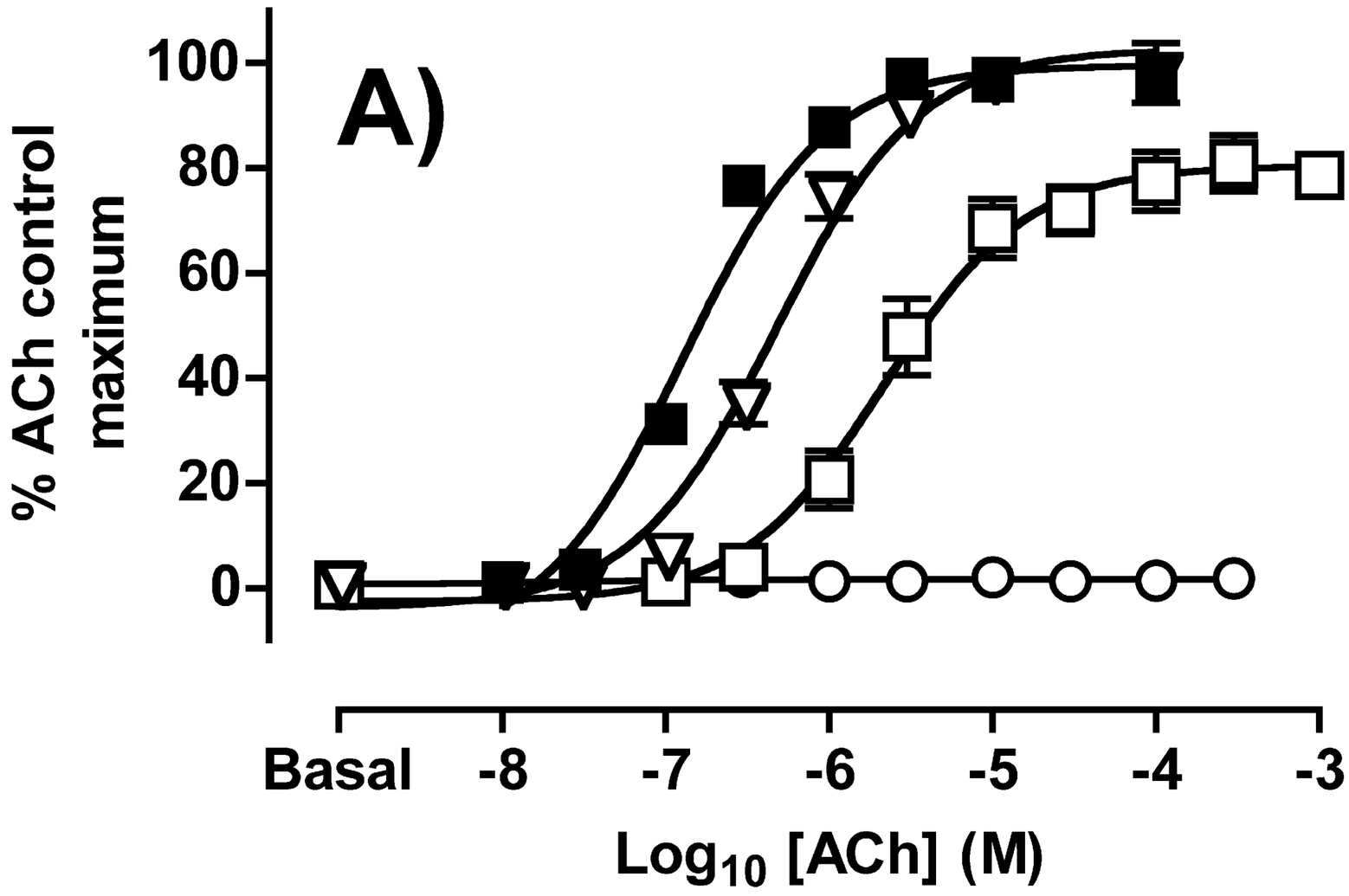

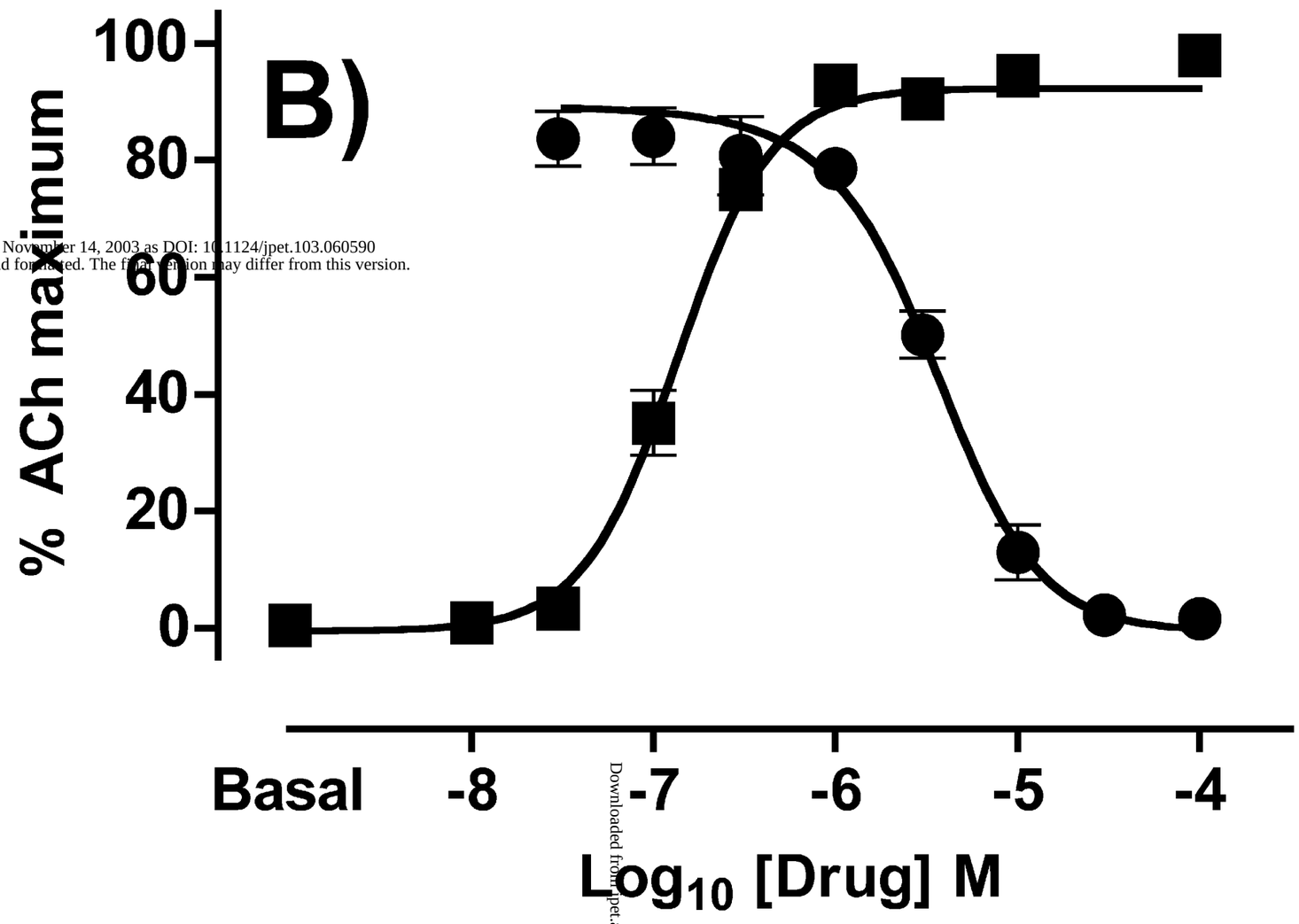

Figure 7